

# Single versus poly-crystalline layered oxide cathode materials for solid-state battery applications - a short review article

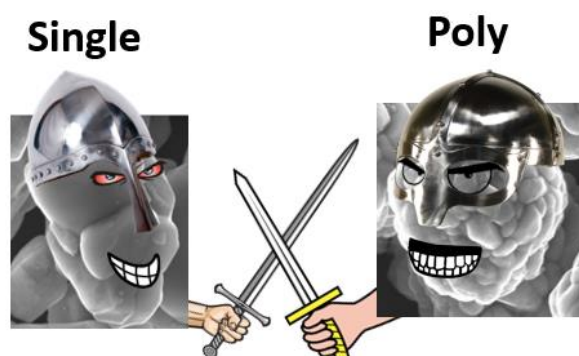
Seyedhosein Payandeh<sup>1,\*</sup>, Damian Goonetilleke<sup>1</sup>, Matteo Bianchini<sup>1,2</sup>, Jürgen Janek<sup>1,3</sup>, Torsten Brezesinski<sup>1,\*</sup>

<sup>1</sup>Battery and Electrochemistry Laboratory (BELLA), Institute of Nanotechnology, Karlsruhe Institute of Technology (KIT), Hermann-von-Helmholtz-Platz 1, 76344 Eggenstein-Leopoldshafen, Germany.

<sup>2</sup>BASF SE, Carl-Bosch-Strasse 38, 67056 Ludwigshafen, Germany.

<sup>3</sup>Institute of Physical Chemistry & Center for Materials Research (ZfM/LaMa), Justus-Liebig-University Giessen, Heinrich-Buff-Ring 17, 35392 Giessen, Germany.

Email: [seyedhosein.payandeh@kit.edu](mailto:seyedhosein.payandeh@kit.edu), [torsten.brezesinski@kit.edu](mailto:torsten.brezesinski@kit.edu)



## Abstract

The recent achievements following the application of single-crystalline (SC) cathode material in solid-state batteries are discussed in this mini-review. The characteristics of SC and polycrystalline (PC) cathode materials are explored, with emphasis on the kinetic and mechanical properties. The critical factors influencing their performance in liquid electrolyte and solid-state battery cells are investigated. Finally, the advantages and disadvantages of both morphologies are discussed and considerations to ensure a fair comparison between SC and PC cathodes in different systems are raised.

## Introduction

Since their commercialization in 1991, when the first lithium-ion batteries (LIBs) utilizing a  $\text{LiCoO}_2$  (LCO) cathode and graphite anode were introduced into consumer electronics, LIBs have continued to maintain the same fundamental combination of a layered oxide cathode material, a graphite anode and an organic liquid electrolyte. Thanks to significant research and development, the specific energy density at the cell level has increased considerably in the past decades, reaching nearly 300 Wh/kg at the time of writing.[1,2] These advances have been driven by optimization at all stages of cell manufacturing, from electrode preparation to cell assembly. However, the energy density is still largely limited by the cathode material. Thus, most LIB materials research has focused on the identification and development of new cathode materials and compositions and their optimization through chemical doping and surface coatings, often providing additional benefits to cycle life and cell reliability.[3–5] One area that has received relatively limited attention until recently is the particle morphology of the cathode material. Conventionally, the production of industrial quantities of cathode materials is carried out using co-precipitation reactions to produce hydroxide precursors of the desired composition, which are then lithiated during annealing to produce the final material. This co-precipitation process, when properly engineered and controlled in stirred reactors, typically results in the characteristic morphology of commercial cathode materials, consisting of spherical secondary particles assembled from agglomerated primary (single-crystalline) grains.[6] However, with the current trend toward cathode material compositions of high Ni content and/or the use of high cutoff voltages, issues with particle fracture have become more prominent and present a significant limitation in both LIBs and solid-state batteries (SSBs). This arises from the random crystallographic orientation of the primary grains, resulting in mechanical stresses between the particles as they expand/contract anisotropically relative to one another upon Li insertion/extraction.[7] This issue is further exacerbated if the Ni content in the cathode is increased, because Ni-rich materials reach greater states of delithiation during charge and therefore undergo larger lattice (volume) changes.[8]

Recently, there have been numerous reports of significant improvements to cycle life in Ni-rich cathode materials achieved by adopting a single-crystalline (SC) morphology.[9] These materials are not true individual single crystals, but can instead be more accurately described as consisting of large (2-3  $\mu\text{m}$ ) monolithic grains, which are more or less de-agglomerated. By eliminating the grain boundaries present in poly-crystalline (PC) materials, these materials do not show intergranular fracture, contributing to an improved cycle life.[10] Despite the benefits,

it should be noted that by their nature, it might be harder to arrange/dense-pack irregularly shaped single crystals, which has some effect on the specific and volumetric capacity of the cathode material when it is incorporated into a cell stack. Moreover, the synthesis of SC materials (requiring fine control over the morphology) is generally more demanding than for PC materials.[11,12] Although several studies have compared PC and SC electrodes of the same chemical composition, it cannot be generalized as to whether the change in morphology brings about improvements in tap density or reduces it.[12–14] For a fair assessment, it is therefore important to consider that SC particles are usually not of comparable size and shape to the spherical particles of PC materials. SC particles are larger than the primary particles of PC materials, but smaller than the secondary ones, leading to different mechanical and kinetic behavior.

While numerous studies of SC materials in LIBs have been recently reported,[10,15–20] a few authors have also investigated their performance in SSBs. To minimize the number of variables, this mini-review will focus on only intercalation-type  $\text{Li}_{1+x}(\text{Ni}_{1-y-z}\text{Co}_y\text{X}_z)_{1-x}\text{O}_2$  [with X = Al (NCA), Mn (NCM)] cathode materials that are considered as the most promising for high-energy SSBs.[21,22]

SSBs may consist of different kinds of solid electrolytes (SEs), such as oxides, polymers, hydroborates, sulfides and halides, with each electrolyte having its own challenges.[23] Oxides are brittle materials, requiring high-temperature sintering, and are vulnerable to crack formation due to volume changes upon cycling.[24,25] Polymers usually show a low ionic conductivity at ambient temperature and have a narrow electrochemical stability window, making them incompatible with high-voltage cathodes.[26,27] Hydroborates are challenging to synthesize and demonstrate better performance for sodium-ion batteries.[28–32] Halides have a high (electrochemical) oxidative stability, but suffer from moderate ionic conductivity and low reductive stability.[33–35] Sulfides (thiophosphates) have a limited chemical and electrochemical stability, however, the decomposition products formed at the interfaces often allow for long-term cycling of high-voltage cathodes. In addition, coating of the cathode material impedes interfacial side reactions. Because of the relatively low cost of sulfide-based electrolytes and their favorable processability, most studies on SC cathodes in SSBs are using this class of SEs.[22,36] Thus, in this mini-review, we summarize the recent reports on the performance of SC cathode materials in SSBs with sulfide electrolytes and attempt to reconcile the benefits and drawbacks of this new morphology compared to PC cathodes. Finally, we

discuss the characteristics of the cathode that must be carefully controlled to achieve a fair comparison between SC and PC materials.

### **Comparison of cracking behavior and electrochemical performance in SSBs**

SC materials offer high mechanical strength, allowing the cathode morphology to be maintained upon cell assembly. During this process, pressures of >100 MPa are typically applied to ensure adequate contact between SE and cathode composite while also reducing the porosity. Liu *et al.* and Doerrer *et al.* have reported the deformation, cracking of secondary particles and fracturing along the grain boundaries for PC cathodes.[37,38] However, both studies showed that the SC cathode material remained intact during the assembly under pressures of up to 1020 MPa. The details of these studies, including the SE used and operating conditions, are summarized in **Table 1**.

SC cathodes also show a more stable electrochemical performance and less cracking with cycling (**Figure 1a,b**). Especially for high-Ni compositions, a cutoff voltage of ~4.3 V vs. Li<sup>+</sup>/Li leads to deep delithiation (beyond 80%), where the so-called H2-H3 phase transition occurs, causing internal strain and large unit-cell shrinkage, with  $\Delta V/V \approx -10\%$  in the extreme case of LiNiO<sub>2</sub> (LNO).[39–41] Crystallographically, SC and PC materials are equivalent and undergo the same transformations. However, the severe anisotropic volume change and lattice mismatch between adjacent primary grains in PC materials during charge and discharge lead to the observed secondary particle fracture. In contrast, this issue is alleviated in SC materials with monolithic grains.

Conforto *et al.* have recently calculated the lithium-diffusion pathway ( $L_{diff}$ ) for SC and PC NCM composite cathodes in SSBs by fitting the impedance data collected during cycling. A considerable increase in  $L_{diff}$  was observed for PC cathodes (by a factor of 3 to 4 after 40 cycles). On the other hand, SC cathodes showed less changes in the mean value of  $L_{diff}$  (by a factor of <2, see **Figure 1c,d**).[42] The increase in  $L_{diff}$  in the PC material is attributed to the hindered transport of lithium in the cathode composite because of secondary particle fracture and subsequent contact loss.

In addition to the effect of volume changes, Han *et al.* discussed the contribution of SE decomposition on cracking. Sulfide-based electrolytes have a narrow stability window, and the oxidative decomposition of argyrodite Li<sub>6</sub>PS<sub>5</sub>Cl at the interface with the cathode material is reported to follow a volume contraction that may accelerate the pulverization of the secondary

particles.[43] Thus, they should be used with coated cathode materials,[44] or use SEs with a higher oxidative stability, such as halides.[45] However, the (crystallographic) density of the SEs needs to be considered. Sulfide-based electrolytes typically have a low density (e.g.  $1.86 \text{ g/cm}^3$  for  $\text{Li}_6\text{PS}_5\text{Cl}$ ), allowing cathode material contents of 70 wt% in the electrode to provide sufficient contact between SE and cathode particles. On the other hand, halides have a higher density (e.g.  $2.43 \text{ g/cm}^3$  for  $\text{Li}_3\text{YCl}_6$ ), requiring a higher gravimetric content of SE (40 wt%) in the cathode to provide sufficient volume fraction and proper contact between SE and cathode particles. Consequently, a lower cathode material content of 60 wt% is proposed as a strategy to achieve stable (long-term) performance.[43]

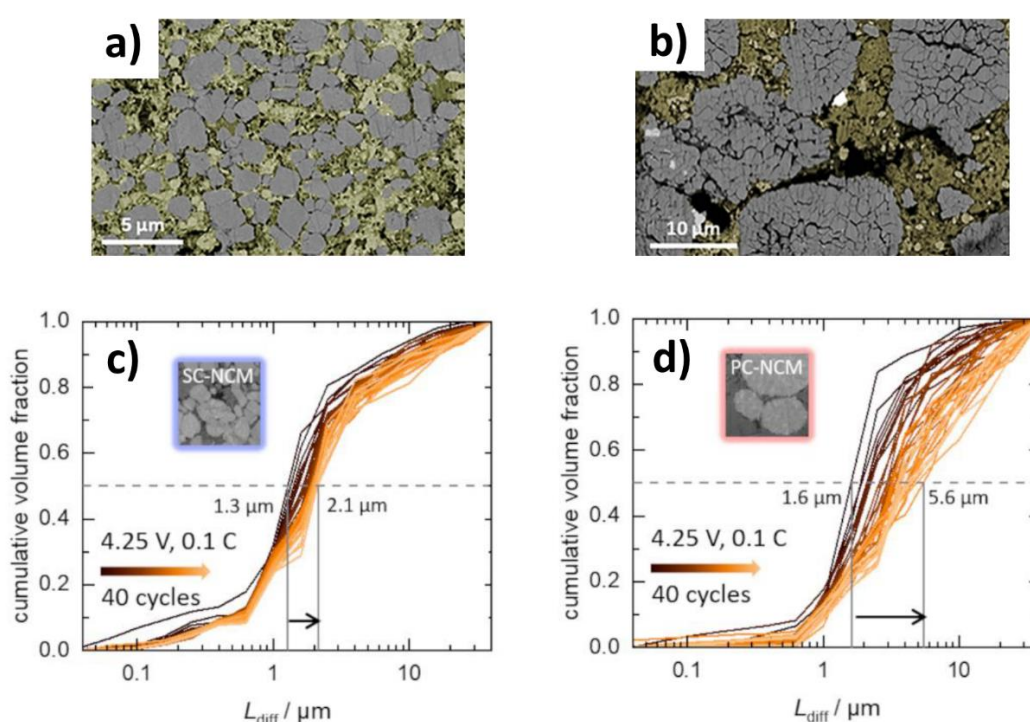


**Figure 1.** Cross-sectional scanning electron microscopy-backscattered electron images of a) SC and b) PC NCA 881101 cathodes after 100 cycles (charged to 4.3 V vs.  $\text{Li}^+/\text{Li}$ ).[43] Reprinted with the permission of Wiley-VCH. Evolution of  $L_{\text{diff}}$  in c) SC and d) PC NCM 811 cathodes. The SSB cells were charged to 4.25 V vs.  $\text{Li}^+/\text{Li}$  and  $L_{\text{diff}}$  was determined by fitting impedance data.[42] Reprinted with the permission of IOP Publishing.

As discussed above, intergranular cracks form mainly at high voltages in PC cathode materials because of large volume changes and the random orientation of primary particles, resulting in non-uniform expansion and contraction along the grain boundaries. Liquid electrolyte can infiltrate into these cracks and utilize the increased surface area of the cathode particles. The

shorter diffusion pathways in the cracked particles cause an apparent increase in lithium-diffusion coefficient ( $D_{\text{Li}}$ , see **Figure 2a**). On the other hand, SC cathodes with fewer grain boundaries are less prone to intragranular cracking and repeated cycling or overcharging can only cause slight fractures.[10,46,47]. However, this comes at the expense of a higher  $L_{\text{diff}}$  in liquid electrolyte-based battery systems because of the larger primary particles. In fact, Trevisanello *et al.* have recently observed kinetic limitations and lower apparent  $D_{\text{Li}}$  for large, uncracked SC cathodes in LIBs (**Figure 2a**).[48]

The observed performance in SSBs, however, is contrary to liquid systems. When PC materials fracture, SE cannot fill the voids and the contact loss between cathode material and SE particles is detrimental, leading to slower kinetics and losses in capacity (**Figure 2b**). On the other hand, in crack-free SC cathodes, the SE stays connected with the cathode particles. Additionally, the lower number of grain boundaries, offering continuous lithium-transport channels, is beneficial to the lithium diffusivity in SSBs.[49] Thus, for the reasons discussed above, in several studies that compare the performance of SC and PC cathodes in SSBs, the SC one showed counter-intuitively faster kinetics. Similar  $D_{\text{Li}}$  values were observed in the initial charge cycle for SC and PC cathodes, with slightly higher  $D_{\text{Li}}$  for the former, especially at higher voltages where the particles start to fracture. However, in the following discharge cycle, the SC cathode showed a much better performance in SSBs, which can be attributed to the cracking and contact loss upon first charging for the PC cathode (**Figure 2b**).[37,49]

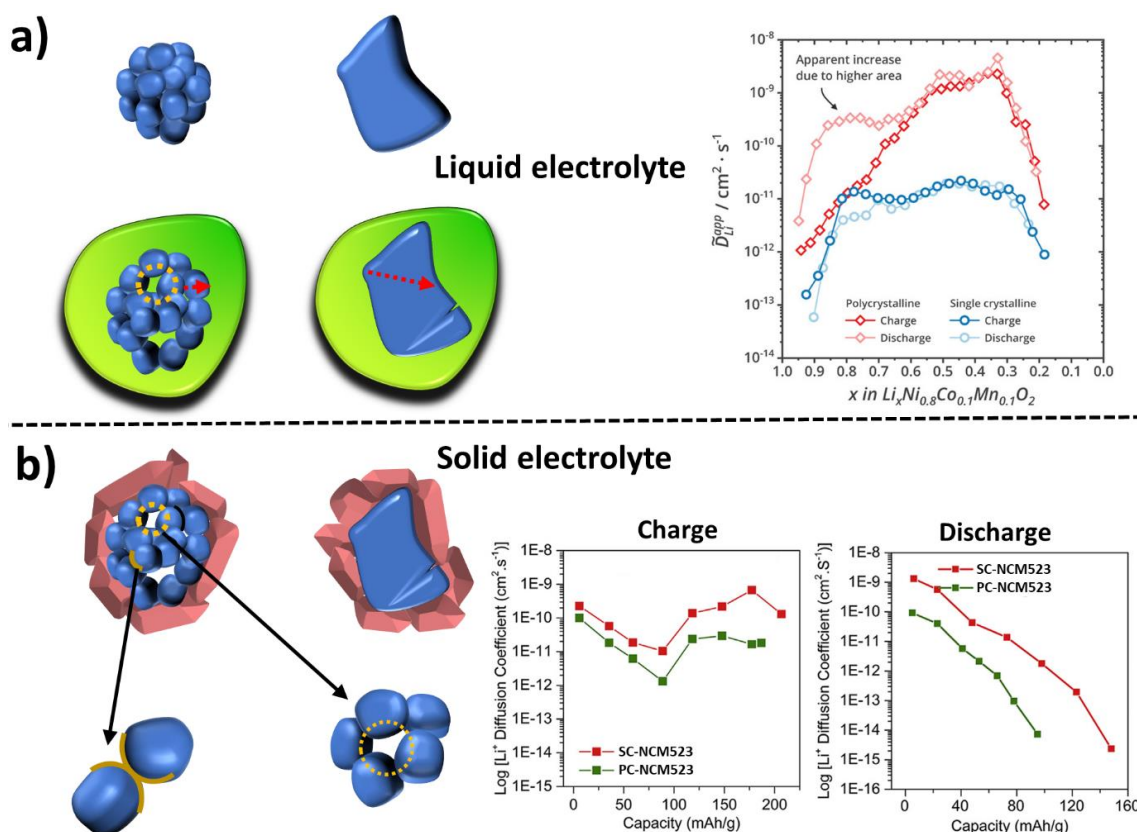


**Figure 2.** Schematic illustration of PC and SC cathodes and the effect of particle fracture and grain boundaries. Apparent lithium-diffusion coefficient ( $\tilde{D}_{Li}^{app}$ ) for the initial charge/discharge cycle of NCM-based cathodes with a) liquid electrolyte (for NCM 811) and b) solid electrolyte (for NCM 523).[48,49] Reprinted with the permissions of Wiley-VCH and Elsevier.

The differing chemo-mechanical behavior of these materials also has implications for the electrochemical performance when applied in SSBs. Previously reported results suggest that adopting a SC morphology is beneficial to the performance.[37,43,49,50] **Table 1** summarizes the characteristics of the reported cells using SC and PC composite cathodes. Liu *et al.* observed similar initial specific capacities of  $\sim 150$  mAh/g and retentions ( $> 80\%$ ) for PC and SC NCM 811 cycled to 4.15 V vs.  $\text{Li}^+/\text{Li}$ . However, increasing the cutoff voltage to 4.35 V vs.  $\text{Li}^+/\text{Li}$  led to a higher specific capacity ( $\sim 185$  mAh/g) and more stable performance for the SC cathode (**Figure 3a**).[37] As mentioned above, Ni-rich NCM materials, such as NCM 811, undergo a phase transition, H2-H3, at around 4.2 V vs.  $\text{Li}^+/\text{Li}$ , accompanied by  $\sim 6\%$  absolute volume change (**Figure 3b,c**). No severe volume changes or cracking were observed when limiting the cutoff voltage on charge, so PC and SC cathodes can show comparable long-term cycling

performance under these conditions (**Figure 3a**). However, increasing the voltage resulted in pronounced volume changes and particle fracture and therefore accelerated capacity fading.

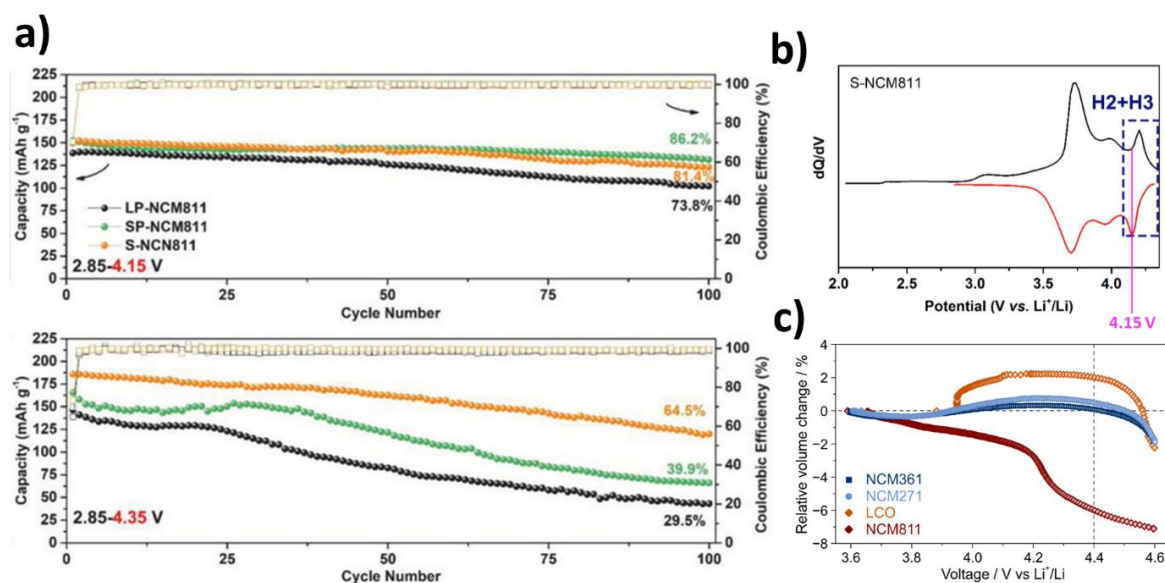


**Figure 3.** a) The effect of cutoff voltage on the long-term cycling behavior of SSBs with SC and PC NCM 811. b) The differential capacity plot for the SC NCM811 cell.[37] Reprinted with the permission of Wiley-VCH. c) Relative unit-cell volume changes for different layered oxide cathode materials.[8] Reprinted with the permission of ACS.

### Considerations for controlling cathode morphology in SSBs

The discussion above outlines some of the advantages of SC cathodes in SSBs. However, given that the morphological differences are more influential for the electrochemical behavior of SC cathodes when used in SSBs compared to LIBs, we believe specific criteria should be considered to have a fair comparison between PC and SC cathodes.

#### 1. Particle size

The specific capacities achieved in NCM-based SSBs are dependent on the particle size of the cathode material. Cathodes with particle size < 10  $\mu\text{m}$  are suggested for SSBs, offering a larger surface area to ensure good contact between particles and improved cathode utilization.[51] However, the cathode utilization in solid-state composites is controlled by the percolation and the important factor is likely the ratio of cathode material to SE particle size to maximize their contact area. Thus, using smaller particle size SE is suggested as a strategy when large cathode particles are used.[52] A mixture of SE particles of various sizes is also suggested to be

advantageous for minimizing void space between particles in cathode composites and improving the electrochemical properties.[53] Additionally, the influence of the cathode particle size on the diffusion needs to be considered. Assuming an average  $D_{\text{Li}}$  of  $5 \times 10^{-12} \text{ cm}^2/\text{s}$ , only particles of radius ( $L$ )  $\sim 6 \text{ }\mu\text{m}$  can be lithiated within a time window ( $t_{\text{dis}}$ ) of 20 h (C/20,  $L < \sqrt{t_{\text{dis}} \times D_{\text{Li}}}$ ). For larger particle sizes, a considerable fraction of the cathode may not be fully (de-)lithiated in the SSB cell. Note that  $D_{\text{Li}} = 5 \times 10^{-12} \text{ cm}^2/\text{s}$  is used because of the strong drop in  $D_{\text{Li}}$  for the lithiated state of NCM.[42] In general, SC cathodes consist of relatively small particles and small-size PC materials should be used to eliminate the size effect when comparing the performance of SC versus PC cathodes. Moreover, SEs of similar particle size should be used to have the same percolation effect.

## 2. Surface characteristics

$\text{Li}_2\text{CO}_3$  and  $\text{LiOH}$  [and NiO-like (rocksalt-type) phases] are known surface impurities in both SC and PC cathodes. For a fair comparison between the two morphologies, cathodes with structurally and chemically similar surfaces should be considered. One strategy is to reconstruct the surface by removing the impurities. Washing is a commonly used method to eliminate impurities (lithium residuals), but studies have shown that water induces  $\text{Li}^+/\text{H}^+$  exchange, leading to the formation of a NiOOH-type surface layer.[50,54] Thus, ethanol as a washing agent is suggested, having a lower solubility for  $\text{Li}_2\text{CO}_3$  and causing less depleted regions.[50] Another study proposes the lithiation of the Ni-rich, rocksalt-type layer by redepositing lithium into the surface lattice (referred to as surface chemistry regulation). Specifically, the NCM material is calcined at high temperatures and under  $\text{O}_2$  flow in the presence of  $\text{LiOH}$  to restore the layered oxide structure at the interface, thereby improving the electrochemical performance.[55]

## 3. Coatings

The application of various coatings to the surface of cathode material particles has been proven in numerous studies to significantly enhance the interfacial stability and therefore the electrochemical performance of SSBs.[56–58] However, the distribution and effectiveness of different coating methods is also largely dependent on the material morphology. Thus, the differences between PC and SC cathodes when subjected to coating processes should be considered. Surface coating of PC cathodes is primarily performed on the secondary particle level. In this case, when the secondary particles fracture, the uncoated primary grains get in direct contact with the electrolyte and decomposition at the interface takes place. This is much

more severe for liquid systems, where the pulverized particles have intimate contact with the liquid electrolyte and coating of the primary particles has been shown to significantly improve the electrochemical performance.[59,60] However, in SSBs, where the contact between cathode material and SE particles is limited and the cracking of secondary particles causes contact loss, the coating of primary particles does not seem to be more beneficial. Nevertheless, it is important to note that in the case of SC cathodes, the coating acts as a primary particle coating that prevents SE decomposition (and particle fracture). Thus, PC cathodes with a coating on both the primary and secondary particles are suggested to be compared with coated SC cathodes.

Additionally, the composition of the coating needs to be controlled precisely.  $\text{LiNbO}_3$  is the most widely used coating material for NCM cathodes in SSBs.[61] Recent reports have shown that the performance is also dependent on the carbonate content of the cathode particles. The best performance has been achieved when a hybrid (niobate/carbonate) coating is formed.[62,63] Thus, SC and PC cathodes with similar carbonate contents and coating chemistries are recommended for comparison.

### **Concluding remarks and outlook**

As many researchers turn their attention toward the next generation of solid-state lithium-ion batteries, the importance of reproducible and reliable comparisons between cathode materials destined for use in SSB systems increases. While many efforts have been directed toward improving the ionic conductivity and interfacial stability of SEs, comparatively less research has been directed toward understanding how modifying the morphology affects the behavior of cathode materials with an SE compared to a liquid electrolyte. In this mini-review, several considerations for evaluating the mechanical and electrochemical behavior of SC cathode materials compared to their PC counterparts have been highlighted. Recent studies in SSBs have shown that adopting a SC morphology reduces the tendency to induce cracking during cycling compared to PC cathodes, where the primary grains' random orientation results in mechanical stresses between the particles. The minor cracking of SC cathodes in SSBs allows proper contact of the cathode material and SE particles to be maintained and leads to improved lithium transport in the composite (higher  $D_{\text{Li}}$ ). This contrasts with the shorter diffusion pathways and higher  $D_{\text{Li}}$  for cracked PC cathodes obtained in LIBs. These findings from the recent studies highlighted in this mini-review clearly demonstrate that while the tremendous

amount of research on cathodes for LIBs provides a thorough foundation for their application in SSBs, the morphology of the cathode material has additional implications because of the nature of the solid-solid interfaces. The use of SC cathodes shows great promise for further improving the viability of SSB systems and it is hoped that the considerations raised above can help to direct future research in this area.

**Table 1.** Overview of the electrochemical performance of SC and PC NCM and NCA cathodes in SBBs.

Cathode material	Coating material	Solid electrolyte	Anode	Particle size (D <sub>50</sub> ) / $\mu\text{m}$	First-cycle specific discharge capacity / mAh/g	Initial Coulombic efficiency / %	Capacity retention / % (cycles)	Active material loading / $\text{mg}/\text{cm}^2$	Temp. / $^{\circ}\text{C}$	Voltage range / V vs. Li <sup>+</sup> /Li	C-rate	Ref.
SC-NCM622	LiNbO <sub>3</sub>	Li <sub>9.54</sub> Si <sub>1.74</sub> P <sub>1.44</sub> S <sub>11.7</sub> Cl <sub>0.3</sub>	Li-In	~3	161 175.7	- 88.7	91.3 (100)	10.2	40	2.7-4.3	C/2 C/10	[64]
SC-NCM523	LiNb <sub>0.5</sub> Ta <sub>0.5</sub> O <sub>3</sub>	Li <sub>10</sub> GeP <sub>2</sub> S <sub>12</sub>	In	3.8	156.4	86.9	~60 (150)	10.7	r.t.	2.5-4.4	C/10	[49]
PC-NCM523	LiNb <sub>0.5</sub> Ta <sub>0.5</sub> O <sub>3</sub>	Li <sub>10</sub> GeP <sub>2</sub> S <sub>12</sub>	In	4.2	127.5	-	~48 (150)	10.7	r.t.	2.5-4.4	C/10	
SC-NCM523	LiNb <sub>0.5</sub> Ta <sub>0.5</sub> O <sub>3</sub>	Li <sub>10</sub> GeP <sub>2</sub> S <sub>12</sub>	Li-In	~3	161.4 139.8	85.8 -	- ~63 (500)	8.4	r.t.	2.5-4.4	C/10 C/3	[65]
SC-NCM811	LiNbO <sub>3</sub>	Li <sub>10</sub> SnP <sub>2</sub> S <sub>12</sub>	Li <sub>4</sub> Ti <sub>5</sub> O <sub>12</sub>	2.8	153	-	79.7 (100)	5.1	30	2.85-4.35	C/3	[37]
SC-NCM811	-	Li <sub>10</sub> SnP <sub>2</sub> S <sub>12</sub>	Li <sub>4</sub> Ti <sub>5</sub> O <sub>12</sub>	2.8	187	74	64.5 (100)	5.1	30	2.85-4.35	C/10	
PC-NCM811	-	Li <sub>10</sub> SnP <sub>2</sub> S <sub>12</sub>	Li <sub>4</sub> Ti <sub>5</sub> O <sub>12</sub>	2.8	165	67.9	39.9 (100)	5.1	30	2.85-4.35	C/10	
SC-NCA801505	-	Li <sub>6</sub> PS <sub>5</sub> Cl	Li-In	-	- 174	- -	94 (200)	~10.5	25	2.6-4.3	C/2 C/10	[50]
PC-NCA801505	-	Li <sub>6</sub> PS <sub>5</sub> Cl	Li-In	-	- 130	- -	~78 (200)	~10.5	25	2.6-4.3	C/2 C/10	
SC-NCM831106	LiNbO <sub>3</sub>	Li <sub>6</sub> PS <sub>5</sub> Cl	Li	3.4	204	85	99.4 (10)	14	30	2.5-4.3	C/15	[38]
PC-NCM831106	LiNbO <sub>3</sub>	Li <sub>6</sub> PS <sub>5</sub> Cl	Li	5.4	152	70	-	14	30	2.5-4.3	C/11	
SC-NCM831106	LiNbO <sub>3</sub>	Li <sub>6</sub> PS <sub>5</sub> Cl	Li <sub>4</sub> Ti <sub>5</sub> O <sub>12</sub>	3.4	~150	-	96.3 (50)	14	30	2.5-4.3	C/6	
PC-NCM831106	LiNbO <sub>3</sub>	Li <sub>6</sub> PS <sub>5</sub> Cl	Li <sub>4</sub> Ti <sub>5</sub> O <sub>12</sub>	5.4	~115	-	92.4 (50)	14	30	2.5-4.3	C/4.4	
SC-NCM811	-	Li <sub>6</sub> PS <sub>5</sub> Cl	Li-In	-	~183*	- 84*	91 (100)	11	25	2.6-4.25	C/10 C/20	[42]
PC-NCM811	-	Li <sub>6</sub> PS <sub>5</sub> Cl	Li-In	-	~153*	- 77*	48 (100)	11		2.6-4.25	C/10 C/20	
SC-NCA881101	-	Li <sub>3</sub> YCl <sub>6</sub>	Li-In	2.8	~180* 199	- 89.6	96.8 (200)	11.3	30	3-4.3*	C/2 C/10	[43]
PC-NCA881101	-	Li <sub>3</sub> YCl <sub>6</sub>	Li-In	11.9	~180* 191	80.6 ~80*	68 (200)*	11.3	30	3-4.3*	C/2 C/10	
SC-NCA881101	-	Li <sub>2</sub> ZrCl <sub>6</sub>	Li-In	-	~182 206	- 85.8	91.3 (100)	-	30	3-4.3*	C/2 C/10	[66]
SC-NCM622	Li <sub>3</sub> BO <sub>3</sub>	Ta-doped LLZO	Li	2	138.8	~80	~57 (50)	1-1.5	80	2.8-4.3	C/20	[67]
SC-NCM622	Li <sub>3</sub> BO <sub>3</sub>	Ta-doped LLZO	Li	10-15	~12*	-	-	1-1.5	80	2.8-4.3	C/20	

\*Interpolated from graphs.

## Acknowledgements

This study was supported by BASF SE.

## References

- [1] G.E. Blomgren, The development and future of lithium ion batteries, *J. Electrochem. Soc.* 164 (2017) A5019–A5025. <https://doi.org/10.1149/2.0251701jes>.
- [2] Y. Liu, R. Zhang, J. Wang, Y. Wang, Current and future lithium-ion battery manufacturing, *IScience*. 24 (2021) 102332. <https://doi.org/10.1016/j.isci.2021.102332>.
- [3] A. Hebert, E. McCalla, The role of metal substitutions in the development of Li batteries, part I: cathodes, *Mater. Adv.* 2 (2021) 3474–3518. <https://doi.org/10.1039/d1ma00081k>.
- [4] A. Manthiram, A reflection on lithium-ion battery cathode chemistry, *Nat. Commun.* 11 (2020) 1550. <https://doi.org/10.1038/s41467-020-15355-0>.
- [5] D. Weber, Đ. Tripković, K. Kretschmer, M. Bianchini, T. Brezesinski, Surface modification strategies for improving the cycling performance of Ni-rich cathode materials, *Eur. J. Inorg. Chem.* 2020 (2020) 3117–3130. <https://doi.org/10.1002/ejic.202000408>.
- [6] H. Dong, G.M. Koenig Jr., A review on synthesis and engineering of crystal precursors produced via coprecipitation for multicomponent lithium-ion battery cathode materials, *CrystEngComm*. 22 (2020) 1514–1530. <https://doi.org/10.1039/c9ce00679f>.
- [7] Z. Ren, X. Zhang, M. Liu, J. Zhou, S. Sun, H. He, D. Wang, Constant dripping wears away a stone: fatigue damage causing particles' cracking, *J. Power Sources*. 416 (2019) 104–110. <https://doi.org/10.1016/j.jpowsour.2019.01.084>.
- [8] F. Strauss, L. de Biasi, A.-Y. Kim, J. Hertle, S. Schweidler, J. Janek, P. Hartmann, T. Brezesinski, Rational design of quasi-zero-strain NCM cathode materials for minimizing volume change effects in all-solid-state batteries, *ACS Materials Lett.* 2 (2020) 84–88. <https://doi.org/10.1021/acsmaterialslett.9b00441>.
- [9] J. Langdon, A. Manthiram, A perspective on single-crystal layered oxide cathodes for lithium-ion batteries, *Energy Storage Mater.* 37 (2021) 143–160. <https://doi.org/10.1016/j.ensm.2021.02.003>.
- [10] G. Qian, Y. Zhang, L. Li, R. Zhang, J. Xu, Z. Cheng, S. Xie, H. Wang, Q. Rao, Y. He,

- Y. Shen, L. Chen, M. Tang, Z.-F. Ma, Single-crystal nickel-rich layered-oxide battery cathode materials: synthesis, electrochemistry, and intra-granular fracture, *Energy Storage Mater.* 27 (2020) 140–149. <https://doi.org/10.1016/j.ensm.2020.01.027>.
- [11] A. Liu, N. Zhang, J.E. Stark, P. Arab, H. Li, J.R. Dahn, Synthesis of Co-free Ni-rich single crystal positive electrode materials for lithium ion batteries: part I. two-step lithiation method for Al- or Mg-doped  $\text{LiNiO}_2$ , *J. Electrochem. Soc.* 168 (2021) 040531. <https://doi.org/10.1149/1945-7111/abf7e8>.
- [12] A. Cao, A. Manthiram, Shape-controlled synthesis of high tap density cathode oxides for lithium ion batteries, *Phys. Chem. Chem. Phys.* 14 (2012) 6724–6728. <https://doi.org/10.1039/c2cp40209b>.
- [13] H. Liu, R. Younesi, K. Edström, Synthesis of single crystalline Ni-rich NMC811 cathode materials and improved performance enabled by ultrathin surface coating layer, *ECS Meet. Abstr.* MA2019-02 (2019) 326. <https://doi.org/10.1149/ma2019-02/5/326>.
- [14] Z. Zhong, L. Chen, S. Huang, W. Shang, L. Kong, M. Sun, L. Chen, W. Ren, Single-crystal  $\text{LiNi}_{0.5}\text{Co}_{0.2}\text{Mn}_{0.3}\text{O}_2$ : a high thermal and cycling stable cathodes for lithium-ion batteries, *J. Mater. Sci.* 55 (2020) 2913–2922. <https://doi.org/10.1007/s10853-019-04133-z>.
- [15] R. Liang, Z.-Y. Wu, W.-M. Yang, Z.-Q. Tang, G.-G. Xiong, Y.-C. Cao, S.-R. Hu, Z.-B. Wang, A simple one-step molten salt method for synthesis of micron-sized single primary particle  $\text{LiNi}_{0.8}\text{Co}_{0.1}\text{Mn}_{0.1}\text{O}_2$  cathode material for lithium-ion batteries, *Ionics.* 26 (2020) 1635–1643. <https://doi.org/10.1007/s11581-020-03500-0>.
- [16] X. Kong, Y. Zhang, S. Peng, J. Zeng, J. Zhao, Superiority of single-crystal to polycrystalline  $\text{LiNi}_x\text{Co}_y\text{Mn}_{1-x-y}\text{O}_2$  cathode materials in storage behaviors for lithium-ion batteries, *ACS Sustainable Chem. Eng.* 8 (2020) 14938–14948. <https://doi.org/10.1021/acssuschemeng.0c05011>.
- [17] H. Li, J. Li, N. Zaker, N. Zhang, G.A. Botton, J.R. Dahn, Synthesis of single crystal  $\text{LiNi}_{0.88}\text{Co}_{0.09}\text{Al}_{0.03}\text{O}_2$  with a two-step lithiation method, *J. Electrochem. Soc.* 166 (2019) A1956–A1963. <https://doi.org/10.1149/2.0681910jes>.
- [18] H. Li, J. Li, X. Ma, J.R. Dahn, Synthesis of single crystal  $\text{LiNi}_{0.6}\text{Mn}_{0.2}\text{Co}_{0.2}\text{O}_2$  with enhanced electrochemical performance for lithium ion batteries, *J. Electrochem. Soc.* 165 (2018) A1038–A1045. <https://doi.org/10.1149/2.0951805jes>.

- [19] L. Wang, B. Wu, D. Mu, X. Liu, Y. Peng, H. Xu, Q. Liu, L. Gai, F. Wu, Single-crystal  $\text{LiNi}_{0.6}\text{Co}_{0.2}\text{Mn}_{0.2}\text{O}_2$  as high performance cathode materials for Li-ion batteries, *J. Alloys Compd.* 674 (2016) 360–367. <https://doi.org/10.1016/j.jallcom.2016.03.061>.
- [20] T. Kimijima, N. Zettsu, K. Yubuta, K. Hirata, K. Kami, K. Teshima, Molybdate flux growth of idiomorphic  $\text{Li}(\text{Ni}_{1/3}\text{Co}_{1/3}\text{Mn}_{1/3})\text{O}_2$  single crystals and characterization of their capabilities as cathode materials for lithium-ion batteries, *J. Mater. Chem. A* 4 (2016) 7289–7296. <https://doi.org/10.1039/c6ta01593j>.
- [21] Y.-G. Lee, S. Fujiki, C. Jung, N. Suzuki, N. Yashiro, R. Omoda, D.-S. Ko, T. Shiratsuchi, T. Sugimoto, S. Ryu, J.H. Ku, T. Watanabe, Y. Park, Y. Aihara, D. Im, I.T. Han, High-energy long-cycling all-solid-state lithium metal batteries enabled by silver–carbon composite anodes, *Nat. Energy* 5 (2020) 299–308. <https://doi.org/10.1038/s41560-020-0575-z>.
- [22] S. Randau, D.A. Weber, O. Kötz, R. Koerver, P. Braun, A. Weber, E. Ivers-Tiffée, T. Adermann, J. Kulisch, W.G. Zeier, F.H. Richter, J. Janek, Benchmarking the performance of all-solid-state lithium batteries, *Nat. Energy* 5 (2020) 259–270. <https://doi.org/10.1038/s41560-020-0565-1>.
- [23] Z. Wu, Z. Xie, A. Yoshida, Z. Wang, X. Hao, A. Abudula, G. Guan, Utmost limits of various solid electrolytes in all-solid-state lithium batteries: a critical review, *Renew. Sustain. Energy Rev.* 109 (2019) 367–385. <https://doi.org/10.1016/j.rser.2019.04.035>.
- [24] R. Grissa, S. Payandeh, M. Heinz, C. Battaglia, Impact of protonation on the electrochemical performance of  $\text{Li}_7\text{La}_3\text{Zr}_2\text{O}_{12}$  garnets, *ACS Appl. Mater. Interfaces* 13 (2021) 14700–14709. <https://doi.org/10.1021/acsami.0c23144>.
- [25] Q. Liu, Z. Geng, C. Han, Y. Fu, S. Li, Y.-b. He, F. Kang, B. Li, Challenges and perspectives of garnet solid electrolytes for all solid-state lithium batteries, *J. Power Sources* 389 (2018) 120–134. <https://doi.org/10.1016/j.jpowsour.2018.04.019>.
- [26] P. Yao, H. Yu, Z. Ding, Y. Liu, J. Lu, M. Lavorgna, J. Wu, X. Liu, Review on polymer-based composite electrolytes for lithium batteries, *Front. Chem.* 7 (2019) 522. <https://doi.org/10.3389/fchem.2019.00522>.
- [27] S. Sen, E. Trevisanello, E. Niemöller, B.-X. Shi, F.J. Simon, F.H. Richter, The role of polymers in lithium solid-state batteries with inorganic solid electrolytes, *J. Mater. Chem. A* 9 (2021) 18701–18732. <https://doi.org/10.1039/d1ta02796d>.

- [28] S. Payandeh, R. Asakura, P. Avramidou, D. Rentsch, Z. Łodziana, R. Černý, A. Remhof, C. Battaglia, Nido-borate/closo-borate mixed-anion electrolytes for all-solid-state batteries, *Chem. Mater.* 32 (2020) 1101–1110. <https://doi.org/10.1021/acs.chemmater.9b03933>.
- [29] L. Duchêne, A. Remhof, H. Hagemann, C. Battaglia, Status and prospects of hydroborate electrolytes for all-solid-state batteries, *Energy Storage Mater.* 25 (2020) 782–794. <https://doi.org/10.1016/j.ensm.2019.08.032>.
- [30] R. Asakura, D. Reber, L. Duchêne, S. Payandeh, A. Remhof, H. Hagemann, C. Battaglia, 4 V room-temperature all-solid-state sodium battery enabled by a passivating cathode/hydroborate solid electrolyte interface, *Energy Environ. Sci.* 13 (2020) 5048–5058. <https://doi.org/10.1039/D0EE01569E>.
- [31] M. Brighi, F. Murgia, R. Černý, Closo-hydroborate sodium salts as an emerging class of room-temperature solid electrolytes, *Cell Rep. Phys. Sci.* 1 (2020) 100217. <https://doi.org/10.1016/j.xcrp.2020.100217>.
- [32] S. Payandeh, D. Rentsch, Z. Łodziana, R. Asakura, L. Bigler, R. Černý, C. Battaglia, A. Remhof, Nido-hydroborate-based electrolytes for all-solid-state lithium batteries, *Adv. Funct. Mater.* 31 (2021) 2010046. <https://doi.org/10.1002/adfm.202010046>.
- [33] X. Li, J. Liang, X. Yang, K.R. Adair, C. Wang, F. Zhao, X. Sun, Progress and perspectives on halide lithium conductors for all-solid-state lithium batteries, *Energy Environ. Sci.* 13 (2020) 1429–1461. <https://doi.org/10.1039/c9ee03828k>.
- [34] S.Y. Kim, K. Kaup, K.-H. Park, A. Assoud, L. Zhou, J. Liu, X. Wu, L.F. Nazar, Lithium ytterbium-based halide solid electrolytes for high voltage all-solid-state batteries, *ACS Materials Lett.* 3 (2021) 930–938. <https://doi.org/10.1021/acsmaterialslett.1c00142>.
- [35] L.M. Riegger, R. Schlem, J. Sann, W.G. Zeier, J. Janek, Lithium-metal anode instability of the superionic halide solid electrolytes and the implications for solid-state batteries, *Angew. Chem. Int. Ed.* 133 (2021) 6792–6797. <https://doi.org/10.1002/ange.202015238>.
- [36] Q. Zhang, D. Cao, Y. Ma, A. Natan, P. Aurora, H. Zhu, Sulfide-based solid-state electrolytes: synthesis, stability, and potential for all-solid-state batteries, *Adv. Mater.* 31 (2019) 1901131. <https://doi.org/10.1002/adma.201901131>.
- [37] X. Liu, B. Zheng, J. Zhao, W. Zhao, Z. Liang, Y. Su, C. Xie, K. Zhou, Y. Xiang, J. Zhu, H. Wang, G. Zhong, Z. Gong, J. Huang, Y. Yang, Electrochemo-mechanical effects on

- structural integrity of Ni-rich cathodes with different microstructures in all solid-state batteries, *Adv. Energy Mater.* 11 (2021) 2003583. <https://doi.org/10.1002/aenm.202003583>.
- [38] C. Doerrler, I. Capone, S. Narayanan, J. Liu, C.R.M. Grovenor, M. Pasta, P.S. Grant, High energy density single-crystal NMC/Li<sub>6</sub>PS<sub>5</sub>Cl cathodes for all-solid-state lithium metal batteries, *ACS Appl. Mater. Interfaces.* 13 (2021) 37809–37815. <https://doi.org/10.1021/acsami.1c07952>.
- [39] M. Bianchini, M. Roca-Ayats, P. Hartmann, T. Brezesinski, J. Janek, There and back again—the journey of LiNiO<sub>2</sub> as a cathode active material, *Angew. Chem. Int. Ed.* 58 (2019) 10434–10458. <https://doi.org/10.1002/anie.201812472>.
- [40] M. Mock, M. Bianchini, F. Fauth, K. Albe, S. Sicolo, Atomistic understanding of the LiNiO<sub>2</sub>-NiO<sub>2</sub> phase diagram from experimentally guided lattice models, *J. Mater. Chem. A.* 9 (2021) 14928–14940. <https://doi.org/10.1039/d1ta00563d>.
- [41] L. de Biasi, A. Schiele, M. Roca-Ayats, G. Garcia, T. Brezesinski, P. Hartmann, J. Janek, Phase transformation behavior and stability of LiNiO<sub>2</sub> cathode material for Li-ion batteries obtained from in situ gas analysis and operando X-ray diffraction, *ChemSusChem.* 12 (2019) 2240–2250. <https://doi.org/10.1002/cssc.201900032>.
- [42] G. Conforto, R. Ruess, D. Schröder, E. Trevisanello, R. Fantin, F.H. Richter, J. Janek, Editors' choice—quantification of the impact of chemo-mechanical degradation on the performance and cycling stability of NCM-based cathodes in solid-state Li-ion batteries, *J. Electrochem. Soc.* 168 (2021) 070546. <https://doi.org/10.1149/1945-7111/ac13d2>.
- [43] Y. Han, S.H. Jung, H. Kwak, S. Jun, H.H. Kwak, J.H. Lee, S.-T. Hong, Y.S. Jung, Single- or poly-crystalline Ni-rich layered cathode, sulfide or halide solid electrolyte: which will be the winners for all-solid-state batteries?, *Adv. Energy Mater.* 11 (2021) 2100126. <https://doi.org/10.1002/aenm.202100126>.
- [44] Y. Zhu, X. He, Y. Mo, Origin of outstanding stability in the lithium solid electrolyte materials: insights from thermodynamic analyses based on first-principles calculations, *ACS Appl. Mater. Interfaces.* 7 (2015) 23685–23693. <https://doi.org/10.1021/acsami.5b07517>.
- [45] K. Kim, D. Park, H.-G. Jung, K.Y. Chung, J.H. Shim, B.C. Wood, S. Yu, Material design strategy for halide solid electrolytes Li<sub>3</sub>MX<sub>6</sub> (X = Cl, Br, and I) for all-solid-state high-

- voltage Li-ion batteries, *Chem. Mater.* 33 (2021) 3669–3677. <https://doi.org/10.1021/acs.chemmater.1c00555>.
- [46] H.-H. Ryu, B. Namkoong, J.-H. Kim, I. Belharouak, C.S. Yoon, Y.-K. Sun, Capacity fading mechanisms in Ni-rich single-crystal NCM cathodes, *ACS Energy Lett.* 6 (2021) 2726–2734. <https://doi.org/10.1021/acsenerylett.1c01089>.
- [47] S. Klein, P. Bärmann, O. Fromm, K. Borzutzki, J. Reiter, Q. Fan, M. Winter, T. Placke, J. Kasnatscheew, Prospects and limitations of single-crystal cathode materials to overcome cross-talk phenomena in high-voltage lithium ion cells, *J. Mater. Chem. A* 9 (2021) 7546–7555. <https://doi.org/10.1039/d0ta11775g>.
- [48] E. Trevisanello, R. Ruess, G. Conforto, F.H. Richter, J. Janek, Polycrystalline and single crystalline NCM cathode materials—quantifying particle cracking, active surface area, and lithium diffusion, *Adv. Energy Mater.* 11 (2021) 2003400. <https://doi.org/10.1002/aenm.202003400>.
- [49] C. Wang, R. Yu, S. Hwang, J. Liang, X. Li, C. Zhao, Y. Sun, J. Wang, N. Holmes, R. Li, H. Huang, S. Zhao, L. Zhang, S. Lu, D. Su, X. Sun, Single crystal cathodes enabling high-performance all-solid-state lithium-ion batteries, *Energy Storage Mater.* 30 (2020) 98–103. <https://doi.org/10.1016/j.ensm.2020.05.007>.
- [50] R. Fantin, E. Trevisanello, R. Ruess, A. Pokle, G. Conforto, F.H. Richter, K. Volz, J. Janek, Synthesis and postprocessing of single-crystalline  $\text{LiNi}_{0.8}\text{Co}_{0.15}\text{Al}_{0.05}\text{O}_2$  for solid-state lithium-ion batteries with high capacity and long cycling stability, *Chem. Mater.* 33 (2021) 2624–2634. <https://doi.org/10.1021/acs.chemmater.1c00471>.
- [51] F. Strauss, T. Bartsch, L. De Biasi, A.Y. Kim, J. Janek, P. Hartmann, T. Brezesinski, Impact of cathode material particle size on the capacity of bulk-type all-solid-state batteries, *ACS Energy Lett.* 3 (2018) 992–996. <https://doi.org/10.1021/acsenerylett.8b00275>.
- [52] T. Shi, Q. Tu, Y. Tian, Y. Xiao, L.J. Miara, O. Kononova, G. Ceder, High active material loading in all-solid-state battery electrode via particle size optimization, *Adv. Energy Mater.* 10 (2020) 1902881. <https://doi.org/10.1002/aenm.201902881>.
- [53] C. Park, S. Lee, K. Kim, M. Kim, S. Choi, D. Shin, Electrochemical properties of composite cathode using bimodal sized electrolyte for all-solid-state batteries, *J. Electrochem. Soc.* 166 (2019) A5318–A5322. <https://doi.org/10.1149/2.0481903jes>.

- [54] D. Pritzl, T. Teufl, A.T.S. Freiberg, B. Strehle, J. Sicklinger, H. Sommer, P. Hartmann, H.A. Gasteiger, Editors' choice—washing of nickel-rich cathode materials for lithium-ion batteries: towards a mechanistic understanding, *J. Electrochem. Soc.* 166 (2019) A4056–A4066. <https://doi.org/10.1149/2.1351915jes>.
- [55] F. Zhang, S. Lou, S. Li, Z. Yu, Q. Liu, A. Dai, C. Cao, M.F. Toney, M. Ge, X. Xiao, W.-K. Lee, Y. Yao, J. Deng, T. Liu, Y. Tang, G. Yin, J. Lu, D. Su, J. Wang, Surface regulation enables high stability of single-crystal lithium-ion cathodes at high voltage, *Nat. Commun.* 11 (2020) 3050. <https://doi.org/10.1038/s41467-020-16824-2>.
- [56] D. Cao, Y. Zhang, A.M. Nolan, X. Sun, C. Liu, J. Sheng, Y. Mo, Y. Wang, H. Zhu, Stable thiophosphate-based all-solid-state lithium batteries through conformally interfacial nanocoating, *Nano Lett.* 20 (2020) 1483–1490. <https://doi.org/10.1021/acs.nanolett.9b02678>.
- [57] Y. Zhang, X. Sun, D. Cao, G. Gao, Z. Yang, H. Zhu, Y. Wang, Self-stabilized  $\text{LiNi}_{0.8}\text{Mn}_{0.1}\text{Co}_{0.1}\text{O}_2$  in thiophosphate-based all-solid-state batteries through extra LiOH, *Energy Storage Mater.* 41 (2021) 505–514. <https://doi.org/10.1016/j.ensm.2021.06.024>.
- [58] D. Kitsche, Y. Tang, Y. Ma, D. Goonetilleke, J. Sann, F. Walther, M. Bianchini, J. Janek, T. Brezesinski, High performance all-solid-state batteries with a Ni-rich NCM cathode coated by atomic layer deposition and lithium thiophosphate solid electrolyte, *ACS Appl. Energy Mater.* 4 (2021) 7338–7345. <https://doi.org/10.1021/acsaem.1c01487>.
- [59] G.-L. Xu, Q. Liu, K.K.S. Lau, Y. Liu, X. Liu, H. Gao, X. Zhou, M. Zhuang, Y. Ren, J. Li, M. Shao, M. Ouyang, F. Pan, Z. Chen, K. Amine, G. Chen, Building ultraconformal protective layers on both secondary and primary particles of layered lithium transition metal oxide cathodes, *Nat. Energy.* 4 (2019) 484–494. <https://doi.org/10.1038/s41560-019-0387-1>.
- [60] M. Yoon, Y. Dong, J. Hwang, J. Sung, H. Cha, K. Ahn, Y. Huang, S.J. Kang, J. Li, J. Cho, Reactive boride infusion stabilizes Ni-rich cathodes for lithium-ion batteries, *Nat. Energy.* 6 (2021) 362–371. <https://doi.org/10.1038/s41560-021-00782-0>.
- [61] S.P. Culver, R. Koerver, W.G. Zeier, J. Janek, On the functionality of coatings for cathode active materials in thiophosphate-based all-solid-state batteries, *Adv. Energy Mater.* 9 (2019) 1900626. <https://doi.org/10.1002/aenm.201900626>.
- [62] A.-Y. Kim, F. Strauss, T. Bartsch, J.H. Teo, J. Janek, T. Brezesinski, Effect of surface

- carbonates on the cyclability of LiNbO<sub>3</sub>-coated NCM622 in all-solid-state batteries with lithium thiophosphate electrolytes, *Sci. Rep.* 11 (2021) 5367. <https://doi.org/10.1038/s41598-021-84799-1>.
- [63] A.-Y. Kim, F. Strauss, T. Bartsch, J.H. Teo, T. Hatsukade, A. Mazilkin, J. Janek, P. Hartmann, T. Brezesinski, Stabilizing effect of a hybrid surface coating on a Ni-rich NCM cathode material in all-solid-state batteries, *Chem. Mater.* 31 (2019) 9664–9672. <https://doi.org/10.1021/acs.chemmater.9b02947>.
- [64] X. Li, W. Peng, R. Tian, D. Song, Z. Wang, H. Zhang, L. Zhu, L. Zhang, Excellent performance single-crystal NCM cathode under high mass loading for all-solid-state lithium batteries, *Electrochim. Acta.* 363 (2020) 137185. <https://doi.org/10.1016/j.electacta.2020.137185>.
- [65] C. Wang, S. Hwang, M. Jiang, J. Liang, Y. Sun, K. Adair, M. Zheng, S. Mukherjee, X. Li, R. Li, H. Huang, S. Zhao, L. Zhang, S. Lu, J. Wang, C.V. Singh, D. Su, X. Sun, Deciphering interfacial chemical and electrochemical reactions of sulfide-based all-solid-state batteries, *Adv. Energy Mater.* 11 (2021) 2100210. <https://doi.org/10.1002/aenm.202100210>.
- [66] H. Kwak, D. Han, J. Lyoo, J. Park, S.H. Jung, Y. Han, G. Kwon, H. Kim, S.-T. Hong, K.-W. Nam, Y.S. Jung, New cost-effective halide solid electrolytes for all-solid-state batteries: mechanochemically prepared Fe<sup>3+</sup>-substituted Li<sub>2</sub>ZrCl<sub>6</sub>, *Adv. Energy Mater.* 11 (2021) 2003190. <https://doi.org/10.1002/aenm.202003190>.
- [67] X. Guo, L. Hao, Y. Yang, Y. Wang, Y. Lu, H. Yu, High cathode utilization efficiency through interface engineering in all-solid-state lithium-metal batteries, *J. Mater. Chem. A.* 7 (2019) 25915–25924. <https://doi.org/10.1039/c9ta09935b>.

#### Important references

[37]

The effect of cutoff voltage on the cycling stability and cracking behavior of SC and PC cathodes morphologies in SSBs is examined.

[42]

Tracking the length of lithium-diffusion pathways upon cycling PC and SC cathodes in SSBs demonstrates that chemo-mechanical degradation in the composite cathode is the major cause of capacity fading.

[43]

Solid electrolyte (halide and sulfide) effects with PC and SC cathode morphologies are thoroughly investigated.

[48]

The  $D_{Li}$  of PC and SC cathode morphologies in LIBs is examined.

[49]

This article compares the  $D_{Li}$  of SC and PC cathodes in SSBs and discusses the effect of charging and discharging on the evolution of  $D_{Li}$ .

[50]

The effect of impurities on the performance of SC cathodes in SSBs is discussed and strategies for their removal are developed.